Carbohydrate Polymers 102 (2014) 970–977

Contents lists available at ScienceDirect

Carbohydrate Polymers

journal homepage: www.elsevier.com/locate/carbpol

Montmorillonite–chitosan–silver sulfadiazine nanocomposites for topical treatment of chronic skin lesions: *In vitro* biocompatibility, antibacterial efficacy and gap closure cell motility properties

Giuseppina Sandri[a], Maria Cristina Bonferoni[a], Franca Ferrari[a], Silvia Rossi[a], Carola Aguzzi[b], Michela Mori[a], Pietro Grisoli[a], Pilar Cerezo[b], Marika Tenci[a], Cesar Viseras[b,c], Carla Caramella[a,*]

[a] Department of Drug Sciences, University of Pavia, Viale Taramelli 12, 27100 Pavia, Italy
[b] Department of Pharmacy and Pharmaceutical Technology, University of Granada, Campus of Cartuja, Granada, 18071 s/n, Spain
[c] Andalusian Institute of Earth Sciences, CSIC-University of Granada, Armilla, Granada, Spain

ARTICLE INFO

Article history:
Received 10 July 2013
Received in revised form 10 October 2013
Accepted 10 October 2013
Available online 30 October 2013

Keywords:
Montmorillonite chitosan nanocomposites
Silver sulfadiazine
Chronic skin lesions
In vitro wound closure
Antimicrobial properties

ABSTRACT

Silver compounds and especially silver sulfadiazine (AgSD) are reported as effective antimicrobial agents against almost all known bacteria, fungi and some viruses. However, AgSD has been shown to be cytotoxic toward fibroblasts and keratinocytes *in vitro* and consequently to retard wound healing *in vivo*.

The aim of the present work was to evaluate the *in vitro* biocompatibility (cytotoxicity and proliferation), antimicrobial efficacy and cell motility gap closure (assay of wound closure) of MT/CS nanocomposites loaded with silver sulfadiazine (AgSD). It is envisioned to be administered as a powder or a dressing for cutaneous application in the treatment of skin ulcers. The loading of AgSD in MT/CS nanocomposites aimed at preventing the delay in wound healing, by decreasing the cytotoxicity of AgSD and maintaining its antimicrobial properties.

Nanocomposites were prepared by using different amounts of MT (100–2000 mg) and 40 ml of a 1% (w/w) chitosan glutamate aqueous solution. The relative amounts of AgSD and chitosan in the systems were assessed by suitable analytic methods. The nanocomposite prepared using 100 mg of MT was characterized for *in vitro* biocompatibility and proliferation and for wound healing using normal human dermal fibroblasts (NHDF). Antimicrobial properties were evaluated against four reference bacterial strains: *Staphylococcus aureus*, *Streptococcus pyogenes*, *Escherichia coli*, and *Pseudomonas aeruginosa*.

AgSD loaded in the 100 MT/CS nanocomposite showed good *in vitro* biocompatibility and gap closure properties (fibroblasts) and maintained AgSD antimicrobial properties, especially against *P. aeruginosa*, that often complicates skin lesions.

1. Introduction

In the last decade, nanocomposites based on clay minerals and biopolymers for pharmaceutical applications have attracted a great attention (Aguzzi, Cerezo, Viseras, & Caramella, 2007; Chiu & Lin, 2012; Viseras, Aguzzi, Cerezo, & Bedmar, 2008; Viseras, Cerezo, Sanchez, Salcedo, & Aguzzi, 2010). These hybrid materials can, in fact, combine the properties of both inorganic and organic components, such as swelling, water uptake, mechanical properties, thermal behavior, rheology and bioadhesion (Günister, Pestreli, Ünlü, & Güngör, 2007; Khunawattanakul, Puttipipatkhachorn, Rades, & Pongjanyakul, 2008; Lertsutthiwong, Noomun, Khunthon, & Limpanart, 2012; Wu & Wu, 2006). Nanocomposites can be constituted of a variety of biopolymers and clay minerals. Among them, montmorillonite (MT) and chitosan (CS) nanocomposites are of major interest, especially for biomedical (tissue engineering) (Haroun, Gamal-Eldeen, & Harding, 2009; Katti, Katti, & Dash, 2008) and biopharmaceutical (modified release) (Depan, Kumar, & Singh, 2009; Joshi, Kevadiya, Mody, & Bajaj, 2012; Takahashi, Yamada, Kataoka, & Nagasaki, 2005; Wang, Du, & Luo, 2008) applications.

MT is a phyllosilicate clay, consisting of a multilayered structure of Si/Al oxide in multilayer stacks, characterized by a sandwich structure comprising two tetrahedron sheets with an edge-bridged octahedral sheet (general structure 2:1 type). MT possesses a net negative charge due to isomorphous ionic substitutions in the layered structure. This charge is compensated by interlayer cations (mainly Na^+ and Mg^{2+}), which can be exchanged by a variety

* Corresponding author. Tel.: +39 0382 987385; fax: +39 0382 422975.
E-mail addresses: giuseppina.sandri@unipv.it (G. Sandri), carla.caramella@unipv.it (C. Caramella).

0144-8617/$ – see front matter © 2013 Elsevier Ltd. All rights reserved.
http://dx.doi.org/10.1016/j.carbpol.2013.10.029

of organic molecules (Aguzzi et al., 2007). Moreover MT possesses haemostatic and absorbent properties and it is used in wound dressings or systems designed to treat lesions and ulcers (Antelman, Goldsmith, & Lampert, 2011; Salcedo et al., 2012; Vaiana et al., 2011).

CS is a cationic biocompatible polysaccharide that promotes the physiologically ordered dermal regeneration during skin reconstruction, regulating the deposition and faster arrangement of thin collagen fibers. Furthermore, CS has effect on fibroblast activation, supporting the regeneration of the extracellular matrix, facilitating cell migration and stimulating the formation of granulation tissue (Francesko & Tzanov, 2011). Moreover, it has been reported as enhancer of cell proliferation and wound healing (Sandri et al., 2011).

MT/CS nanocomposites were characterized by biocompatibility, good proliferation properties and biodegradability. In a previous work of ours, MT/CS nanocomposites biocompatibility was assessed by means of *in vitro* cytotoxicity and cell proliferation tests carried out on Caco-2 cell cultures, chosen as representative of intestinal cells, in view of oral administration of the nanocomposites and intestinal drug delivery (Salcedo et al., 2012). Such nanocomposites determined a progressive reduction of wound area in an *in vitro* wound healing model, indicating an effective enhancement of Caco-2 proliferation. The biohybrid material, derived from the interaction between MT and CS, demonstrated therefore promising properties for pharmaceutical applications. Other authors have considered the possible application of MT/CS composite for culture and targeted delivery of mesenchymal stem and regenerative cells (Popryadukhin et al., 2012). In addition, complexes based on CS and delaminated MT showed better cell proliferation, faster degradation rate and better biocompatibility than pure CS (Hsu, Wang, & Lin, 2012).

In a previous work of ours (Aguzzi et al., 2014) a nanocomposite based on MT and CS and loaded with silver sulfadiazine was characterized by solid state analysis. The intercalation of the polymer in the interlayer space of the clay mineral was confirmed by X-ray powder diffraction and FTIR analysis. The morphology study by high resolution transmission electron microscopy indicated that clay dispersion within the polymer matrix was relatively homogeneous. The results confirmed the formation of well dispersed ordered intercalated assemble layers of montmorillonite in chitosan matrix. The presence of AgSD in intercalated three-dimensional nanocomposite internal structures was confirmed by energy-dispersion X-ray analysis. The amount of drug retained was calculated both by TGA and elemental analysis. Solid state characterization of loaded and unloaded nanocomposites confirmed the effective interaction between the organic and inorganic components and the successful drug loading of clay/chitosan nanostructures.

Given these premises, the aim of the present work was to evaluate the *in vitro* biocompatibility (cytotoxicity and proliferation), antimicrobial efficacy and cell motility gap closure (assay of wound closure) of MT/CS nanocomposites loaded with silver sulfadiazine (AgSD). It is envisioned to be administered as a powder or a dressing for cutaneous application in the treatment of skin ulcers.

Silver is commonly employed to prevent or to treat wound infections that could impair healing, and also to prevent infections of severe lesions (burn and chronic skin lesions) in presence of antibiotic-resistant bacteria (Bergin & Wraight, 2006; Lipsky & Hoey, 2009; Ranzato, Martinotti, Volante, Mazzucco, & Burlando, 2010; Wasiak et al., 2008). In fact, silver has been proposed as an effective antimicrobial agent due to its ability to strongly interact with thiolic groups present in the respiratory enzymes of the bacterial cell. Additionally, silver has been proven to interact with structural proteins and preferentially to bind with DNA bases to inhibit replication (Bergin & Wraight, 2006). For these reasons, silver is reported as effective against almost all known bacteria including fungi and some viruses (Bergin & Wraight, 2006). Silver compounds such as silver nitrate and silver sulfadiazine are commonly applied to skin chronic lesions and burns (Bergin & Wraight, 2006) and in particular silver sulfadiazine is considered the gold standard treatment in topical burn (Atiyeh, Costagliola, Hayek, & Dibo, 2007). However, the employment of silver sulfadiazine is controversial as pointed out by Storm-Versloot et al. (2010) because of questionable topical antibacterial efficacy as founded by meta-analyses of silver sulfadiazine clinical studies, and because of delayed wound healing. The delayed wound healing is mainly due to the demonstrated cytotoxicity of silver sulfadiazine (AgSD) toward fibroblasts and keratinocytes *in vitro* and consequent retardation of wound healing *in vivo* (Muller et al., 2003). To decrease the AgSD cytotoxic action and to better exploit its antimicrobial effect without impairing wound healing, AgSD was loaded in MT/CS nanocomposites: chitosan role was fundamental to aid the association between AgSD and MT.

MT/CS/AgSD nanocomposites (ternary systems), prepared by an intercalation technique in aqueous solution have been compared with binary systems based on MT/AgSD and MT/CS as control. The systems have been analyzed for CS and AgSD composition. All the complexes have been characterized for *in vitro* biocompatibility on normal human dermal fibroblasts and for *in vitro* wound healing properties. The antimicrobial properties of the nanocomposites have also been evaluated.

2. Experimental

2.1. Materials

The nanocomposites has been prepared by using:

- clay mineral: pharmaceutical grade montmorillonite (Veegum HS©, VHS) (MT), kindly gifted by Vanderbilt Company (USA);
- chitosan base (CS) (average molar mass = 251,000 g mol^{-1}; viscosity = 12 mPa s evaluated on 1% (w/v) solution in HCl 0.1 M at 90 s^{-1} with rotational rheometer equipped with coaxial cylinders C14 (Bohlin CS, Bohlin Instrument Division, Metrics Group Ltd., UK), containing an average of 1559 glucosamine units (glucosamine molar mass = 161 g mol^{-1}), with 98% deacetylation degree, purchased from Faravelli (I);
- silver sulfadiazine (AgSD) (Sigma Aldrich, I)

2.2. Methods

2.2.1. System preparation

2.2.1.1. MT/CS nanocomposites. CS aqueous solutions (1%, w/w) were prepared by adding glutamic acid in a stoichiometric amount to chitosan base to obtain complete CS salification and solubilization. Known amounts of clay mineral powder (100–2000 mg) were then dispersed in 40 ml CS solution. The resulting dispersions were shaken at 150 rpm for 2 days in a water bath (Falc Instruments, I) at room temperature and the solid phases were subsequently recovered by centrifugation at 5000 rpm for 15 min (mod. 4218 ALC International, I), frozen at −20 °C for 24 h and freeze-dried for 24 h (Heto 15, Analitica De Mori, I). The following nanocomposites were obtained: 100 MT/CS; 200 MT/CS; 500 MT/CS; 1000 MT/CS; 2000 MT/CS (the numbers correspond to the amount of MT employed for the preparation).

2.2.1.2. MT/CS/AgSD nanocomposites. The procedure followed for the preparation of drug loaded nanocomposites was exactly the same followed for MT/CS nanocomposites, except that AgSD

was added to CS solution to achieve 0.02% (w/w) concentration. The following drug loaded nanocomposites were obtained: 100 MT/CS/AgSD; 200 MT/CS/AgSD; 500 MT/CS/AgSD; 1000 MT/CS/AgSD; 2000 MT/CS/AgSD.

2.2.1.3. MT/AgSD complexes. AgSD (0.02%, w/w) solution was prepared in NH_4OH 30% solution. Known amounts of clay mineral powder (100–2000 mg) were then dispersed in 40 ml of AgSD solution. The resulting dispersions were shaken at 150 rpm for 2 days in a water bath (Falc Instruments, I) at room temperature and the solid phases were subsequently recovered by centrifugation at 5000 rpm for 15 min (mod. 4218 ALC International, I) frozen at −20 °C for 24 h and freeze-dried for 24 h (Heto 15, Analitica De Mori, I). The following complexes were obtained: 100 MT/AgSD; 200 MT/AgSD; 500 MT/AgSD; 1000 MT/AgSD; 2000 MT/AgSD.

2.2.2. System characterization

2.2.2.1. System compositions. The effective AgSD and CS amounts in the above described systems were determined by using analytical methods hereafter described.

2.2.2.1.1. AgSD assay. AgSD content was assayed by an HPLC method (USP 35) using a Series 200 apparatus (PerkinElmer, I) equipped with a UV detector set at 254 nm and a C18 column (B10C18*30QS, Microbondapak, Interchrom, Interchim, Stepbio, I). The mobile phase, fluxed at 1 ml/min, was a mixture of water/CH_3CN/phosphoric acid having 900/99/1 volume ratio. A calibration curve was obtained using AgSD standard solutions in the concentration range 1–25 μg/ml. An AgSD stock solution (50 μg/ml) was prepared by using a diluting solution (NH_4OH 30% diluted 1:10 (v/v) with water). The samples were prepared by diluting the stock solution with mobile phase.

The supernatant solution recovered after complex/nanocomposite centrifugation was diluted using mobile phase and assayed.

2.2.2.1.2. Chitosan assay. CS was quantified by means of a ninhydrin assay modified from Leane, Nankervis, Smith, and Illum (2004). A calibration curve was prepared by using chitosan glutamate solutions at the following concentrations: 0.75, 0.5, 0.25 and 0.1 (w/w). To obtain chitosan precipitation, each CS glutamate solution (2 ml) was diluted 1:1 (v/v) with a NaOH 2 M solution. The supernatant was removed by centrifuging each sample at 5000 rpm for 15 min (mod. 4218 ALC International, I). The chitosan precipitate was washed twice with 2 ml of NaOH 2 M. Subsequently CS was solubilized by adding 2 ml of HCl 1 M and adjusting the pH to 5. Each sample was diluted 1:1 (v/v) with 2 ml of the ninhydrin reagent (ninhydrin 2% (w/v), hydrindantin 6.8 mg/l in 3:1 (v/v) DMSO:lithium acetate buffer 4 M, pH 5.2; Sigma–Aldrich, I) under nitrogen blanket. Each sample was placed in a shaking bath at 100 °C for 8 min. The vials were then vortexed for 15 s in order to oxide the hydrindantin excess. After cooling, each sample was diluted 1:10 (v/v) with a 1:1 ethanol:water mixture and the absorbance was assayed at 570 nm (Lamba 25 spectrophotometer, Perkin Elmer, I). The calibration curve was linear in the chitosan glutamate range from 0.75 to 0.1% (w/w) with R^2 values always higher than 0.9995.

2.2.2.2. Biocompatibility and proliferation tests. Normal human dermal fibroblasts (NHDF) from juvenile foreskin (PromoCell GmbH, G) were used. Cells between the 2nd and 5th passage were employed for all the experiments. Fibroblasts were grown in Dulbecco's modified Eagle medium (DMEM, Lonza, I), supplemented with 10% fetal calf serum (FCS, Euroclone, I) and 200 IU/ml penicillin 0.2 mg/ml streptomycin (PBI International, I), kept at 37 °C in a 5% CO_2 atmosphere with 95% relative humidity (RH).

Fibroblasts were seeded in each well of 96-well plates (area 0.34 cm^2) at a density of 10^5 cells/cm^2. Cells were grown 24 h to obtain sub-confluence.

Then cells were washed with saline solution and the cell substrates were put in contact with the samples.

In a first set of experiments MT biocompatibility was assessed after 3 h contact, whereas proliferation was determined after 24 h contact; the MT concentrations assayed in the growth medium ranged from 5 to 300 μg/ml.

Subsequently cell substrates were put in contact with 100 MT/CS/AgSD nanocomposite re-suspended in growth medium at two concentrations, corresponding to 300 μg/ml MT and 10 μg/ml AgSD or 150 μg/ml MT and 5 μg/ml AgSD. 100 MT/AgSD complex and AgSD suspension, both having the same AgSD concentrations (5 or 10 μg/ml), as well as CS 1% (w/w) solution in growth medium, were also examined. The samples were put in contact with the fibroblasts either for 3 (biocompatibility) or 24 h (proliferation). Subsequently, the MTT test was performed. This test is based on the activity of mitochondrial dehydrogenases of vital cells that convert MTT in formazan. 125 μl of MTT solution (Sigma Aldrich, I) at 0.25 μg/ml concentration in HBSS (Hank's Buffered Salt Solution) pH 7.4 was put in contact with each sample for 3 h. The reagent was then removed from each well and the cells were washed with PBS (150 μl) to remove the samples and un-reacted MTT solution. After PBS removal, 100 μl of DMSO was put in each well and the absorbance was assayed at 570 nm by means of an ELISA plate reader (Imark Absorbance Reader, Biorad, I), with a reference wavelength set at 655 nm. Cell viability was calculated as % ratio of the absorbance of each sample and the absorbance of the cells kept in contact with the growth medium (control).

2.2.2.3. Cell motility assay for wound healing. The gap closure cell motility assay is based on the employment of Petri μ-Dish (35 mm, Ibidi, Giardini, I) in which an insert is enclosed (Sandri et al., 2013). The insert is constituted of 2 chambers with a growth area of 0.22 cm^2 divided by a septum with a width of cell free gap of 500 μm ± 50 μm.

Fibroblasts were seeded in each chamber at 10^5 cells/cm^2 concentration and grown at confluence in standard conditions as described in Section 2.2.2.2. After 24 h cells reach confluence and the insert was removed displaying 2 areas of cell substrates divided by the gap. Cell substrates were put in contact with 200 μl of 100 MT/CS or 100 MT/CS/AgSD nanocomposites re-suspended in growth medium at two concentrations, both containing MT at 150 μg/ml and AgSD at 5 μg/ml concentration. Cells kept in contact with growth medium were used as control. At prefixed time intervals (0, 24, 48 h) microphotographs were taken to evaluate the cell growth in the gap.

2.2.2.4. Antibacterial activity. The antimicrobial properties of AgSD loaded nanocomposite, 100 MT/CS nanocomposite, 100 MT/AgSD complex, AgSD and MT suspensions were assessed against the following reference bacterial strains: *Staphylococcus aureus* ATCC 6538, *Streptococcus pyogenes* ATCC 19615, *Escherichia coli* ATCC 10536, *Pseudomonas aeruginosa* ATCC 10145. Before testing, bacteria were grown overnight in Tryptone Soya Broth (Oxoid, UK) at 37 °C. The cultures were the centrifuged at 224 × *g* for 20 min to separate cells from culture broth and suspended in phosphate buffer saline (PBS) at pH 7.3. The suspensions were diluted to adjust the number of cells to 1×10^7–1×10^8 CFU/ml.

The antimicrobial activity was evaluated by means of the microdilution method using 96 microwell plates, according to Clinical and Laboratory Standards Institute procedures (NCCLS, 2003).

All experiments were performed in triplicate. The minimum inhibitory concentration (MIC) was the lowest AgSD concentration that caused 100% inhibition of microbial growth. Minimum

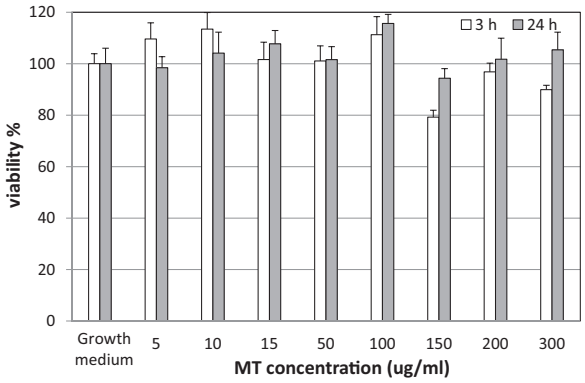

Fig. 1. Biocompatibility (contact time 3 h) and proliferation (contact time 24 h) properties (% viability) of MT at various concentrations toward normal human dermal fibroblasts (mean values ± sd; $n = 8$).

Mann–Whitney (Wilcoxon) *W* test (only the significantly different comparisons are reported).

Contact time 3 h:	Contact time 24 h:
Growth medium *vs* 150 μg/ml; growth medium *vs* 300 μg/ml; 5 *vs* 150 μg/ml; 5 *vs* 300 μg/ml; 10 *vs* 150 μg/ml; 10 *vs* 200 μg/ml; 10 *vs* 300 μg/ml; 15 *vs* 150 μg/ml; 15 *vs* 300 μg/ml; 50 *vs* 150 μg/ml; 100 *vs* 150 μg/ml; 100 *vs* 300 μg/ml; 150 *vs* 200 μg/ml; 150 *vs* 300 μg/ml	Growth medium *vs* 100 μg/ml; 5 *vs* 100 μg/ml; 100 μg/ml *vs* 150 μg/ml

Contact time 3 h *vs* 24 h: 150 μg/ml.

bactericidal concentration (MBC) was the lowest concentration resulting in >99.9% reduction of the initial inoculum. Temperature and incubation time depended on the microbial species.

A twofold serial broth dilution method in Iso-Sensitest broth (ISB, Oxoid, UK) was carried out to determine antibacterial activity against the reference strains. The starting inoculum was 1.0×10^7 CFU/ml. Various concentrations of nanocomposites, complex, AgSD and MT were tested. The incubation temperature was 37 °C; MIC and MBC were detected after 24 h.

2.3. Statistical analysis

Statistical differences were determined according to one-way ANOVA followed by *post hoc* Sheffè test as for the results of system composition are concerned (Stat Graphics 5.0, Statistical Graphics Corporation, MD, USA). For all other measurements statistical differences were evaluated by means of a non-parametric test: Mann Whitney (Wilcolxon) *W* test, (Stat Graphics 5.0, Statistical Graphics Corporation, MD, USA). In both cases differences were considered significant at $p < 0.05$; only significant differences are reported in the captions of the relevant table/figure.

3. Results and discussion

3.1. System composition

The % (w/w) composition of clay/drug complexes (MT/AgSD), clay/polymer (MT/CS) and drug loaded (MT/CS/AgSD) nanocomposites are reported in Table 1. In the case of clay/drug complexes, on increasing MT quantity, the amount of AgSD intercalated into MT sheets remains almost constant (about 4 mg, corresponding to ≅50% of the drug added in the clay suspension). These results can be explained by an equilibrium distribution of the drug between the clay and the outer solution. When considering the clay/polymer (MT/CS) nanocomposites, the amount of CS in the nanocomposite increases on increasing MT/CS ratio: from 49 to 179 mg, corresponding to ≅12 or 45%, respectively, of the chitosan amount added to MT suspension. This confirms the high affinity of chitosan for the clay, as previously reported (Salcedo et al., 2012). On the other hand, the w/w percentage of CS in the clay increases on decreasing MT/CS ratios. XRPD analysis recently carried out on these MT/CS nanocomposites have demonstrated that samples containing higher w/w chitosan percentages are characterized by a greater disorder in the structure, corresponding to a possible exfoliation of clay sheets (Aguzzi et al., 2014). These findings can be applied to explain the behavior of MT/CS nanocomposites here observed and to describe the possible modification induced by a high MT/CS ratio to the clay structure. The exfoliation of MT sheets could in turn determine an incomplete intercalation of polymer chains inside the clay and lead to their partial exposition to the outer space of chitosan with amino groups not involved in interaction with MT and therefore ready for a prompt interaction with other molecules.

The high affinity of CS for MT as well as the availability of a part of polymer chains outside the clay can explain the significantly increasing amounts of AgSD into the drug loaded (MT/CS/AgSD) nanocomposites on decreasing MT/CS ratio. The drug amounts loaded range from 7.1 to 5.2 mg (corresponding to ≅87 or 65% respectively, of the drug added in the MT/CS suspension) and are in all cases significantly higher than those observed for the MT/AgSD complexes containing the same MT amount. The lower the MT/CS ratios in the nanocomposites, the higher the w/w percentage of CS associated with the clay and the loading of AgSD. Drug loading either in terms of amount or w/w percentage is directly related with MT/CS weight ratios. This result can be explained by the occurrence of bonds between Ag^+ and CS aminogroups: these bonds can take place either with the polymer intercalated in the clay sheets, thus favoring the intercalation of the drug itself, or with the polymer chains partially exposed outside these sheets, due to their exfoliation. As a final remark, the rank order of CS w/w percentages is the same for MT/CS and MT/CS/AgSD nanocomposites: this result supports the hypothesis that an exfoliation of MT occurs on decreasing MT/CS ratio and that this phenomenon can explain the trend of AgSD amounts and w/w percentages.

All chitosan chains interactered with phyllosilicate as evidenced by thermal analysis reported in Aguzzi et al. (2014) where it was observed that glutamate counterions were totally replaced by clay.

Thanks to the highest CS and AgSD w/w percentages, the 100 MT/CS/AgSD nanocomposite has been selected as more promising system and has therefore been subjected to the further characterization of biological and antimicrobial properties. Moreover 100 MT/CS/AgSD nanocomposite was characterized by AgSD stability at 25 °C in dark and tight container in N_2 blanket for 3 months (AgSD content = 99.6 ± 0.8%) and low moisture content as

Table 1
Quali-quantitative compositions of MT/CS/AgSD and MT/CS nanocomposites and MT/AgSD complexes (mean values ± sd; $n = 3$).

Sample name	MT		AgSD		CS	
	Amount (mg)	% (w/w)	Amount (mg)	% (w/w)	Amount (mg)	% (w/w)
100 MT/AgSD	100	96.1	4.1 ± 0.009	3.9 ± 0.01		
500 MT/AgSD	500	99.2	4.0 ± 0.003	0.8 ± 0.01		
1000 MT/AgSD	1000	99.6	3.7 ± 0.001	0.4 ± 0.01		
1500 MT/AgSD	1500	99.7	3.9 ± 0.003	0.3 ± 0.01		
2000 MT/AgSD	2000	99.8	4.0 ± 0.010	0.2 ± 0.01		
100 MT/CS	100	67.0			49.2 ± 0.48	33.0 ± 2.82
500 MT/CS	500	86.2			80.0 ± 21.35	13.8 ± 5.55
1000 MT/CS	1000	87.5			142.8 ± 18.11	12.5 ± 2.04
1500 MT/CS	1500	90.5			157.5 ± 19.34	9.5 ± 1.14
2000 MT/CS	2000	91.8			178.6 ± 29.76	8.2 ± 0.59
100 MT/CS/AgSD	100	61.7	7.1 ± 0.05*a	4.4 ± 0.70	54.9 ± 2.85	33.9 ± 1.76
500 MT/CS/AgSD	500	88.4	6.7 ± 0.15*b	1.2 ± 0.20	58.7 ± 7.52	10.4 ± 5.60
1000 MT/CS/AgSD	1000	90.1	5.9 ± 0.10*c	0.5 ± 0.05	104.4 ± 2.70	9.4 ± 1.92
1500 MT/CS/AgSD	1500	91.0	5.5 ± 0.11*d	0.3 ± 0.02	143.6 ± 2.40	8.7 ± 0.15
2000 MT/CS/AgSD	2000	91.8	5.2 ± 0.17*e	0.2 ± 0.01	174.4 ± 12.87	8.0 ± 0.58

evaluated by thermogravimetric analysis (TGA) (Aguzzi et al., 2014): in particular the water loss at 100 °C was equal to 3.4% (w/w) ($n = 3$; standard deviation of 0.003) and at 120 °C 3.86% ($n = 3$; standard deviation of 0.005).

3.2. Biocompatibility and proliferation properties

In Fig. 1 the results (% viability) of biocompatibility and proliferation tests effected on normal human dermal fibroblasts treated with MT suspensions of various concentrations (5–300 μg/ml) are reported.

Both biocompatibility and proliferation of cells are close to 100% and not significantly different from the control (growth medium) for all MT concentrations except the one containing 150 μg/ml MT after 3 h contact. This result indicates that even though MT is not soluble and could therefore precipitate onto the cell substrate, it does not determine cell suffering but allows normal cell growth even after 24 h contact.

Fig. 2 illustrates the results (% viability) of biocompatibility and proliferation tests carried out on normal human dermal fibroblasts in presence of 100 MT/CS nanocomposite suspensions, containing various MT concentrations (150–300 μg/ml).

The intercalation of CS into the MT sheets does not reduce the biocompatibility and proliferation properties of MT that remain close to 100% and are not significantly different from the control (growth medium).

These results enabled us to consider the highest MT concentration (300 μg/ml), as appropriate for the subsequent characterization of the 100 MT/CS/AgSD nanocomposite.

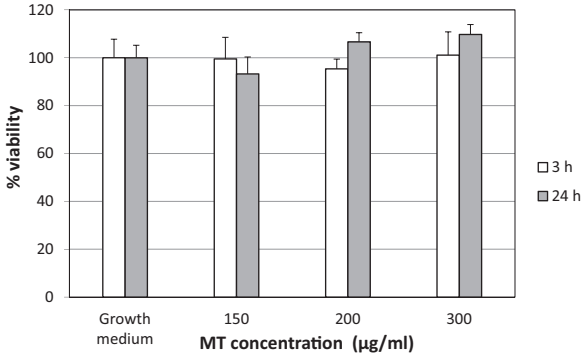

Fig. 2. Biocompatibility (contact time 3 h) and proliferation (contact time 24 h) properties (% viability) of 100 MT/CS nanocomposite at various MT concentrations toward normal human dermal fibroblasts (mean values ± sd; $n = 8$).

Fig. 3 reports the results (% viability) of biocompatibility and proliferation tests performed on normal human dermal fibroblasts in presence of 100 MT/CS/AgSD nanocomposite, AgSD and AgSD/MT suspensions (containing 5 or 10 μg/ml AgSD) and of a CS 1% (w/w) solution.

CS confirms its biocompatibility properties, being characterized by % viability values close or even higher (but not significantly different) than those of the control (growth medium).

AgSD suspensions, at both concentrations, determine poor cell viability after both 3 or 24 h contact time, indicating, as expected, that the drug is not biocompatible and impairs cell growth.

The 100 MT/AgSD complex is slightly less cytotoxic than the corresponding AgSD suspension, as indicated by significantly higher cell viability at both concentrations; however in spite of the improved biocompatibility, cell viability is never higher than 30%. This suggests that the interaction of MT with AgSD is be labile and does not allow cell protection against the AgSD cytotoxic action.

The 100 MT/CS/AgSD nanocomposite, on the contrary, determines higher cell viability values, especially in the proliferation test. Even at the higher AgSD concentration (10 μg/ml) cell viability was 48% and 77% after 3 and 24 h, respectively; these values are significantly higher than those obtained for AgSD and 100 MT/AgSD at the same drug concentration. With the lower AgSD concentration (5 μg/ml) cell viability of the nanocomposite is 92% and 100% after 3 and 24 h, respectively; these values are significantly higher than those of AgSD and 100 MT/AgSD at the same drug concentration and comparable (not significantly different) than those of the growth medium. These results suggest that the nanocomposite is able to protect fibroblasts from the cytotoxic effect of the drug and to allow cell growth in 24 h as the growth medium. The increase in AgSD concentration from 5 to 10 μg/ml, determines a significant decrease of cell viability for the nanocomposite at both contact times and for the 100 MT/AgSD complex after 24 h.

3.3. Cell motility assay for wound healing

In Fig. 4 the results of the gap closure cell motility assay are reported. The microphotographs taken at time 0 evidence for all samples the presence of well defined gaps (mimicking wounds), separating the two areas in which the cells reached confluence. Insoluble clay particles are visible in the substrates treated with MT/CS and drug loaded nanocomposites. After 24 h, fibroblasts start to invade the gaps: the presence of particles does not impair cell growth when treated with both nanocomposites. Even in the case of 100 MT/CS/AgSD, despite the presence of the cytotoxic drug, cells cross the gap and maintain their natural

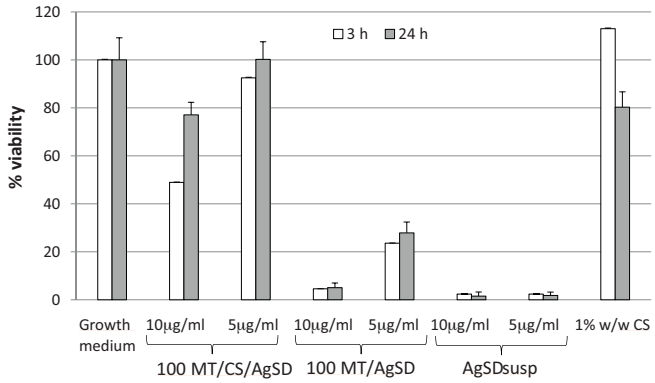

Fig. 3. Biocompatibility (contact time 3 h) and proliferation (contact time 24 h) properties (% viability) toward normal human dermal fibroblasts of 100 MT/CS/AgSD and 100 MT/AgSD nanocomposites and AgSD suspensions (mean values ± sd; $n = 8$).

Mann–Whitney (Wilcoxon) *W* test (only significantly different comparison are reported).

3 h contact time:	24 h contact time:
5 μg/ml	5 μg/ml
Growth medium *vs* MT/AgSD; growth medium *vs* AgSD; MT/CS/AgSD *vs* MT/AgSD; MT/CS/AgSD *vs* AgSD; MT/AgSD *vs* AgSD	Growth medium *vs* MT/AgSD; growth medium *vs* AgSD; MT/CS/AgSD *vs* MT/AgSD; MT/CS/AgSD *vs* AgSD; MT/AgSD *vs* AgSD
10 μg/ml	10 μg/ml
Growth medium *vs* MT/CS/AgSD; growth medium *vs* MT/AgSD; growth medium *vs* AgSD; MT/CS/AgSD *vs* MT/AgSD; MT/CS/AgSD *vs* AgSD	Growth medium *vs* MT/CS/AgSD; growth medium *vs* MT/AgSD; growth medium *vs* AgSD; MT/CS/AgSD *vs* MT/AgSD; MT/CS/AgSD *vs* AgSD; MT/AgSD *vs* AgSD

3 h: 5 *vs* 10 μg/ml of AgSD – MT/CS/AgSD.

24 h: 5 *vs* 10 μg/ml of AgSD – MT/CS/AgSD; MT/AgSD.

stretched out and spindle-like shape. For all the samples fibroblasts completely fill the gap after 48 h; no differences can be evidenced between the control (growth medium) and the two nanocomposites, either drug loaded or not, indicating that their presence does not impair cell proliferation and the normal capability of fibroblasts to cover and fill the gaps by crossing the empty zone and forming anastomosis. These results are in line with those of the biocompatibility and proliferation tests.

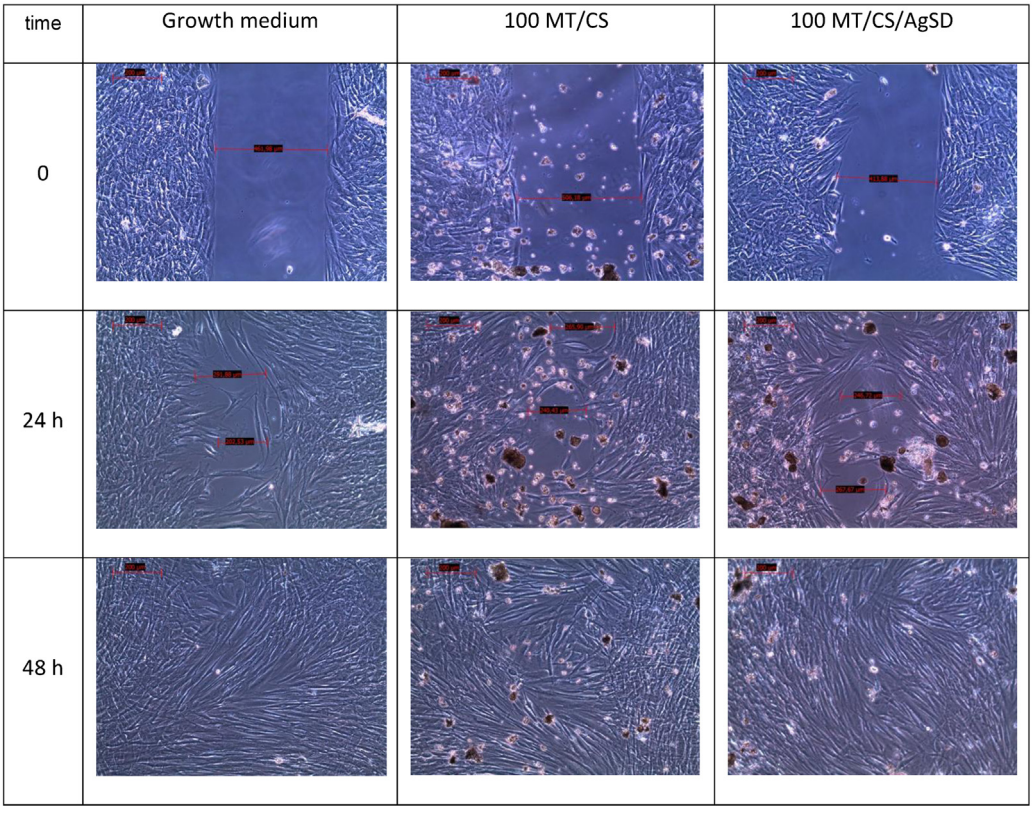

Fig. 4. Microphotographs taken during the gap closure cell motility test at time 0 and after increasing contact times.

Table 2
MIC values of AgSD and AgSD containing samples in comparison with100 MT/CS and MT.

MIC (μg/ml)	*Staphylococcus aureus* ATCC 6538	*Streptococcus pyogenes* ATCC 19615	*Escherichia coli* ATCC 10536	*Pseudomonas aeruginosa* ATCC 10145
MT	>150	>150	>150	>150
100 MT/CS	>150	>150	>150	>150
AgSD	150	75	37.5	37.5
100 MT/AgSD	37.5	18.7	37.5	9.1
100 MT/CS/AgSD	37.5	18.7	18.7	9.1

Table 3
MBC values of AgSD and AgSD containing samples in comparison with100 MT/CS and MT.

MBC (μg/ml)	*Staphylococcus aureus* ATCC 6538	*Streptococcus pyogenes* ATCC 19615	*Escherichia coli* ATCC 10536	*Pseudomonas aeruginosa* ATCC 10145
MT	>150	>150	>150	>150
100 MT/CS	>150	>150	>150	>150
AgSD	>150	75	>150	>150
100 MT/AgSD	>150	37.5	75	>150
100 MT/CS/AgSD	>150	37.5	37.5	37.5

3.4. Antimicrobial properties

The antimicrobial properties, expressed as MIC and MBC values, are reported in Tables 2 and 3, respectively. 100 MT/CS nanocomposite and MT do not show antimicrobial properties. This indicates that neither montmorillonite nor chitosan, when included in montmorillonite sheets, possess antimicrobial activity against the strains considered.

As for MIC values (Table 2) the 100 MT/CS/AgSD nanocomposite and the complex 100 MT/AgSD show MIC values equal or lower than those of the AgSD suspension. This result could be explained by an improved contact between the drug and the microorganisms, determined by the interaction of MT/CS or MT with AgSD at a molecular level, responsible for an increased AgSD surface area and a more intimate contact with the microorganisms. Considering MBC values (Table 3), it can be observed that AgSD is microbicide only against *S. pyogenes*. 100 MT/AgSD complex is characterized by microbicidal activity against *S. pyogenes* at lower concentration than AgSD and is moreover microbicide against *E. coli*. The nanocomposite 100 MT/CS/AgSD shows microbicidal activity against three strains, *S. pyogenes*, *E. coli* and *Pseudomonas aeruginosa*, thus demonstrating to be more effective than AgSD in suspension. As a general remark, the loading of AgSD in MT/CS nanocomposite enhanced antibacterial properties of AgSD.

4. Conclusions

A nanocomposite based on montorillonite and chitosan and loaded with AgSD, having optimal composition of the ingredients has been developed. The 100 MT/CS/AgSD nanocomposite is able to protect fibroblasts from the cytotoxic action of the drug, enabling their proliferation *in vitro*. This result has been confirmed in an *in vitro* wound healing test used as a proof of concept. In particular the AgSD loaded nanocomposite does not impair cell proliferation and the normal capability of fibroblasts to fill an empty gap simulating a wound. AgSD loading into the nanocomposite does not quench the antimicrobial properties of the drug, but improves its bacteriostatic and bactericidal properties, especially against *Pseudomonas aeruginosa*, that often complicates skin lesions. The results of this study indicate that a montmorillonite chitosan silver sulfadiazine nanocomposite should be considered as a promising system for the treatment of skin lesions.

References

Aguzzi, C., Cerezo, P., Viseras, C., & Caramella, C. (2007). Use of clays as drug delivery systems: Possibilities and limitations. *Applied Clay Science*, *36*, 22–36.

Aguzzi, C., Sandri, G., Viseras, C., Bonferoni, M. C., Cerezo, P., Rossi, S., et al. (2014). Solid state characterization of silver sulfadiazine loaded on montmorillonite/chitosan nanocomposite for wound healing. *Colloids and Surfaces B: Biointerfaces*, *113*, 152–157. http://dx.doi.org/10.1016/j.colsurfb.2013.08.043

Antelman, P., Goldsmith, D., & Lampert, S. (2011). *Topical antibiotic formulations*. Patent No. WO 2011/097546 A2.

Atiyeh, B. S., Costagliola, M., Hayek, S. N., & Dibo, S. A. (2007). Effect of silver on burn wound infection control and healing: Review of the literature. *Burns*, *33*, 139–148.

Bergin, S., & Wraight, P. (2006). Silver based wound dressings and topical agents for treating diabetic foot ulcers. *Cochrane Database of Systematic Reviews,*. Art. No.: CD005082.

Chiu, C.-W., & Lin, J.-J. (2012). Self-assembly behavior of polymer-assisted clays. *Progress in Polymer Science*, *37*, 406–444.

Depan, D., Kumar, A. P., & Singh, R. P. (2009). Cell proliferation and controlled drug release studies of nanohybrids based on chitosan-g-lactic acid and montmorillonite. *Acta Biomaterialia*, *5*, 93–100.

Francesko, A., & Tzanov, T. (2011). Chitin, chitosan and derivatives for wound healing and tissue engineering. *Advances in Biochemical Engineering/Biotechnology*, *125*, 1–27.

Günister, E., Pestreli, D., Ünlü, C. H., & Güngör, N. (2007). Synthesis and characterization of chitosan–MMT biocomposite systems. *Carbohydrate Polymers*, *67*, 358–365.

Haroun, A. A., Gamal-Eldeen, A., & Harding, D. R. K. (2009). Preparation, characterization and in vitro biological study of biomimetic three-dimensional gelatin–montmorillonite/cellulose scaffold for tissue engineering. *Journal of Materials Science*, *20*, 2527–2540.

Hsu, S.-H., Wang, M.-C., & Lin, J.-J. (2012). Biocompatibility and antimicrobial evaluation of montmorillonite/chitosan nanocomposites. *Applied Clay Science*, *56*, 53–62.

Joshi, G. V., Kevadiya, B. D., Mody, H. M., & Bajaj, H. C. (2012). Confinement and controlled release of quinine on chitosan–montmorillonite bionanocomposites. *Journal of Polymer Science Part A: Polymer Chemistry*, *50*, 423–430.

Katti, K. S., Katti, D. R., & Dash, R. (2008). Synthesis and characterization of a novel chitosan/montmorillonite/hydroxyapatite nanocomposite for bone tissue engineering. *Biomedical Materials*, *3*, 034122.

Khunawattanakul, W., Puttipipatkhachorn, S., Rades, T., & Pongjanyakul, T. (2008). Chitosan–magnesium aluminum silicate composite dispersions: Characterization of rheology, flocculate size and zeta potential. *International Journal of Pharmaceutics*, *351*, 227–235.

Leane, M. M., Nankervis, R., Smith, A., & Illum, L. (2004). Use of the ninhydrin assay to measure the release of chitosan from oral solid dosage forms. *International Journal of Pharmaceutics*, *271*, 241–249.

Lertsutthiwong, P., Noomun, K., Khunthon, S., & Limpanart, S. (2012). Influence of chitosan characteristics on the properties of biopolymeric chitosan–montmorillonite. *Natural Science: Materials International*, *22*, 502–508.

Lipsky, B. A., & Hoey, C. (2009). Topical antimicrobial therapy for treating chronic wounds. *Clinical Infectious Diseases*, *49*, 1541–1549.

Muller, M. J., Hollyoak, M. A., Moaveni, Z., Brown, T. L. H., Herndon, D. N., & Heggers, J. P. (2003). Retardation of wound healing by silver sulfadiazine is reversed by *Aloe vera* and nystatin. *Burns*, *29*, 834–836.

NCCLS. (2003). Methods for dilution antimicrobial susceptibility tests for bacteria that grow aerobically. In *Approved Standard M7-A6, 6th ed.* Wayne, PA.

Popryadukhin, P. V., Dobrovolskaya, I. P., Yudin, V. E., Mvankova, I. E., Smolyaninov, A. B., & Smirnova, N. V. (2012). Composite materials based on chitosan and montmorillonite prospects for use as matrix for culturing of stem and regenerative cells. *Cell and Tissue Biology*, *6*, 82–88.

Ranzato, E., Martinotti, S., Volante, A., Mazzucco, L., & Burlando, B. (2010). Platelet lysate modulates MMP-2 and MMP-9 expression, matrix deposition and cell-to-matrix adhesion in keratinocytes and fibroblasts. *Experimental Dermatology*, *20*, 308–313.

Salcedo, I., Aguzzi, C., Sandri, G., Bonferoni, M. C., Mori, M., Cerezo, P., et al. (2012). In vitro biocompatibility and mucoadhesion of montmorillonite chitosan nanocomposite: A new drug delivery. *Applied Clay Science*, *55*, 131–137.

Sandri, G., Bonferoni, M. C., D'Autilia, F., Rossi, S., Ferrari, F., Grisoli, P., et al. (2013). Wound dressings based on silver sulfadiazine SLN for tissue repairing. *European Journal of Pharmaceutics and Biopharmaceutics*, *84*, 84–90.

Sandri, G., Bonferoni, M. C., Rossi, S., Ferrari, F., Mori, M., Del Fante, C., et al. (2011). Platelet lysate formulations based on mucoadhesive polymers for the treatment of corneal lesions. *Journal of Pharmacy and Pharmacology*, *63*, 189–219.

Storm-Versloot, M. N., Vos, C. G., Ubbink, D. T., & Vermeulen, H. (2010). Topical silver for preventing wound infection. *Cochrane Database of Systemic Reviews,*. Art No.: CD006478.

Takahashi, T., Yamada, Y., Kataoka, K., & Nagasaki, Y. (2005). Preparation of a novel PEG-clay hybrid as a DDS material: Dispersion stability and sustained release profiles. *Journal of Controlled Release*, *107*, 408–416.

Vaiana, C. A., Leonard, M. K., Drummy, L. F., Singh, K. M., Bubulya, A., Vaia, R. A., et al. (2011). Epidermal growth factor: Layered silicate nanocomposites for tissue regeneration. *Biomacromolecules*, *12*, 3139–3146.

Viseras, C., Aguzzi, C., Cerezo, P., & Bedmar, M. C. (2008). Biopolymer–clay nanocomposites for controlled drug delivery. *Materials Science and Technology*, *24*, 1020–1026.

Viseras, C., Cerezo, P., Sanchez, R., Salcedo, I., & Aguzzi, C. (2010). Current challenges in clay minerals for drug delivery. *Applied Clay Sciences*, *48*, 291–295.

Wang, X., Du, Y., & Luo, J. (2008). Biopolymer/montmorillonite nanocomposite: Preparation, drug-controlled release property and cytotoxicity. *Nanotechnology*, *19*, 065707.

Wasiak, J., Cleland, H., & Campbell, F. (2008). Dressings for superficial and partial thickness burns. *Cochrane Database of Systematic Reviews,*. Art. No.: CD002106.

Wu, T. M., & Wu, C. Y. (2006). Biodegradable poly (lactic acid)/chitosan-modified montmorillonite nanocomposites: Preparation and characterization. *Polymer Degradation and Stability*, *9*, 2198–2204.